Received: 24 January 2022 | Revised: 20 July 2022 | Accepted: 30 August 2022

DOI: 10.1002/ppp.2169

RESEARCH ARTICLE

WILEY

Geographic object-based image analysis (GEOBIA) of the distribution and characteristics of aeolian sand dunes in Arctic Sweden

Melanie Stammler[1] | Thomas Stevens[2] | Daniel Hölbling[3]

[1]Department of Geography, University of Bonn, Bonn, Germany

[2]Department of Earth Sciences, Uppsala University, Uppsala, Sweden

[3]Department of Geoinformatics – Z_GIS, University of Salzburg, Salzburg, Austria

Correspondence
Melanie Stammler, Department of Geography, University of Bonn, Meckenheimer Allee 166, 53115 Bonn, Germany.
Email: stammler@uni-bonn.de

Funding information
Göran Gustafsson Foundation, Grant/Award Number: 1929

Abstract

Current climate change in the Arctic is unprecedented in the instrumental record, with profound consequences for the environment and landscape. In Arctic Sweden, aeolian sand dunes have been impacted by climatic changes since their initial formation after the retreat of the last glacial ice sheet. Dune type, location and orientation can therefore be used to explore past wind patterns and landscape destabilisation in this sensitive area. However, knowledge of the full spatial extent and characteristics of these dunes is limited by their inaccessibility and dense vegetation cover. Geographic object-based image analysis (GEOBIA) permits the semi-automatic creation of reproducible parameter-based objects and can be an appropriate means to systematically and spatially map these dunes remotely. Here, a digital elevation model (DEM) and its derivatives, such as slope and curvature, were segmented in a GEOBIA context, enabling the identification and mapping of aeolian sand dunes in Arctic Sweden. Analysis of the GEOBIA-derived and expert-accepted polygons affirms the prevalence of parabolic dune type and reveals the coexistence of simple dunes with large coalesced systems. Furthermore, mapped dune orientations and relationships to other geomorphological features were used to explore past wind directions and to identify sediment sources as well as the reasons for sand availability. The results indicate that most dune systems in Arctic Sweden were initially supplied by glaciofluvial and fluvial disturbances of sandy esker systems. Topographic control of wind direction is the dominant influence on dune orientation. Further, our approach shows that analysing the GEOBIA-derived dune objects in their geomorphological context paves the way for successfully investigating aeolian sand dune location, type and orientation in Arctic Sweden, thereby facilitating the understanding of post-glacial landscape (in)stability and evolution in the area.

KEYWORDS

geomorphological mapping, Holocene, landscape development, parabolic dunes, semi-automatic landform delimination, wind directions

1 | INTRODUCTION

Climate change has been framed as the defining issue of our time.[1] With the Arctic changing at an unpreceded speed and with knock-on effects for global climate,[2,3] there is a pressing need to improve the understanding of past Arctic environments and landscapes to enhance the robustness of future projections. One archive of past Arctic environment and surface processes is aeolian sand dunes, which are common in Arctic Fennoscandia, especially in Sweden and Finland.[4] As periglacial landforms, dunes in Arctic Sweden tend to be parabolic in type, are part of complex sedimentary associations and coexist with other periglacial landforms, such as eskers and drumlins. Cold-climate dune formation and movement is forced by agents such as wind, temperature and moisture, often via disturbance or changes to vegetation. Variability in dune morphology and reworking is thus a result of a combination of these factors,[5–7] and cold-climate dunes are therefore sensitive indicators of environmental changes.[5,6,8]

Aeolian sand dunes in Arctic Sweden are believed to have initially formed within a few hundred to a thousand years following the last deglaciation,[9] which occurred in this area at c. 10.5–9.9 cal kyr BP.[10] However, radiocarbon and luminescence dating studies conducted on dune sediments in Arctic Finland have revealed multiple episodes of reactivation during the Holocene, as well as inconsistencies over the ages of dune cores.[5,11–14] The reactivation of Fennoscandian Arctic dunes may be related to climate or human-induced fires, or both, which destabilise anchoring vegetation and facilitate dune movement. Analysis of dune stratigraphy in Finland has shown numerous charcoal horizons and buried podsols, indicative of a complex history of Holocene movement that most recently has been linked to abrupt climate changes in the North Atlantic.[12] Today, most dunes in the region are stabilised by forest vegetation, especially Scots pine (*Pinus sylvestrus*) and mountain birch (*Betula pubescens* subsp. tortuosa), as well as *Betula nana*, *Calluna vulgaris*, *Empetrum nigrum* and *Vaccinium vitisidaea* dwarf shrubs above the tree line. Pine invasion into Arctic Finland occurred approximately 9,000 years ago,[15] with pine considered as initial colonising species in Fennoscandia (see[12,16]). Dunes in some areas of Arctic Fennoscandia often exhibit currently active blowouts, indicating periodic, ongoing dune disturbances.[12,17] In addition to recording these periodic disturbances, parabolic dunes can be used as indicators of prevalent sand-transporting wind directions during dune formation of the parabolic form.[18,19]

Previous work on Arctic Fennoscandian dunes has tended to focus on dunes in Finland, and although some links to climate have been proposed, the details of this relationship are debated. Recent research on dunes in Arctic Sweden is lacking. In Sweden, aeolian research was strong in the 1920s (e.g.[20–22]) when a school with a focus on aeolian geomorphology formed in Uppsala.[19] A pause in publications occurred afterwards, with a few exceptions,[4,6,23,24] primarily focused on mapping. Recently, interest in investigating Swedish dunes has grown (e.g.[8,25,26]), although with a primary focus on aeolian sand dunes in central and southern Sweden. A first step in utilising Arctic Swedish aeolian sand dunes to infer climate and landscape development is accurate, consistent, systematic, and has detailed mapping and characterisation.[27] Gaining information about sand dune location and form allows the investigation of wind patterns dominating during dune formation and modification,[18,19] as well as the origins of sand supply and overall driving mechanisms of formation.[28] To date, Arctic Swedish sand dune locations are solely available as point features based on a combination of field data, aerial imagery interpretation[29] and hand-drawn geomorphological maps.[4,23] However, given the large, often inaccessible areas these dunes are found in, and the at-times dense vegetation cover, such point mapping is likely to be incomplete and yields limited spatial information.

While satellite missions such as Landsat have rendered mapping aeolian sand dunes based on remotely sensed data possible, the increased availability of and accessibility to spaceborne data has led to a large variety of quantitative and qualitative analyses of aeolian landforms ([30,31]), featuring manual mapping approaches (e.g.[32,33]) as well as semi-automatic and automatic ones (e.g.[34–36]).

Geographic object-based image analysis (GEOBIA), a semi-automatic mapping approach, permits the creation of reproducible parameter-based polygons, referred to as objects, through segmentation and classification of spatial data.[37–41] In a geomorphological sense, GEOBIA allows for the delimitation of landforms as objects, e.g., alpine landforms,[42] synthetic drumlins[43] and aeolian landforms.[34] Focusing on dunes as objects that represent landforms rather than points, which cannot entail geomorphic information such as shape and orientation, allows for a better interpretation of the spatial differentiation pattern of, e.g., their occurrence or form.[44]

We apply GEOBIA as a means of semi-automatic mapping of Arctic Swedish aeolian sand dunes using digital elevation data to provide insight into the type, location and orientation of the characteristics of aeolian landforms as displayed today, in an area where GEOBIA has not previously been applied. The data set resulting from GEOBIA analysis and expert-acceptance allows for the interpretation of wind directions during parabolic dune formation, geomorphic associations, sand sources and the reasons for sand availability, in short, the causes of dune formation. We thus aim to explore the applicability of object-based mapping for aeolian sand dunes in Arctic Sweden to assess wind dynamics, topographic control, sediment routing and the timing of dune formation, with the overall goal of understanding post-glacial landscape (in)stability and evolution in the area.

2 | STUDY AREA AND REGIONAL SETTING

The main dune fields of Arctic Sweden focused on here lie between 67.7 and 68.5°N in Norrbotten County in Swedish Lapland (part of Sápmi). The area is characterised by higher elevations and steeper slopes in close proximity to the Norwegian border, with the east and south-east of the area characterised by flatter wetlands (Figure 1). Today's landscape of Arctic Sweden shows the extensive impact of previous glaciation (e.g.[10]). Dead ice topography, eskers and drumlin orientations indicate dominant Quaternary ice flow directions towards the south-east.[10,45] Non-flow-parallel drumlins in parts of the area are interpreted as part of a relict, older pre-late last glacial landscape.[45]

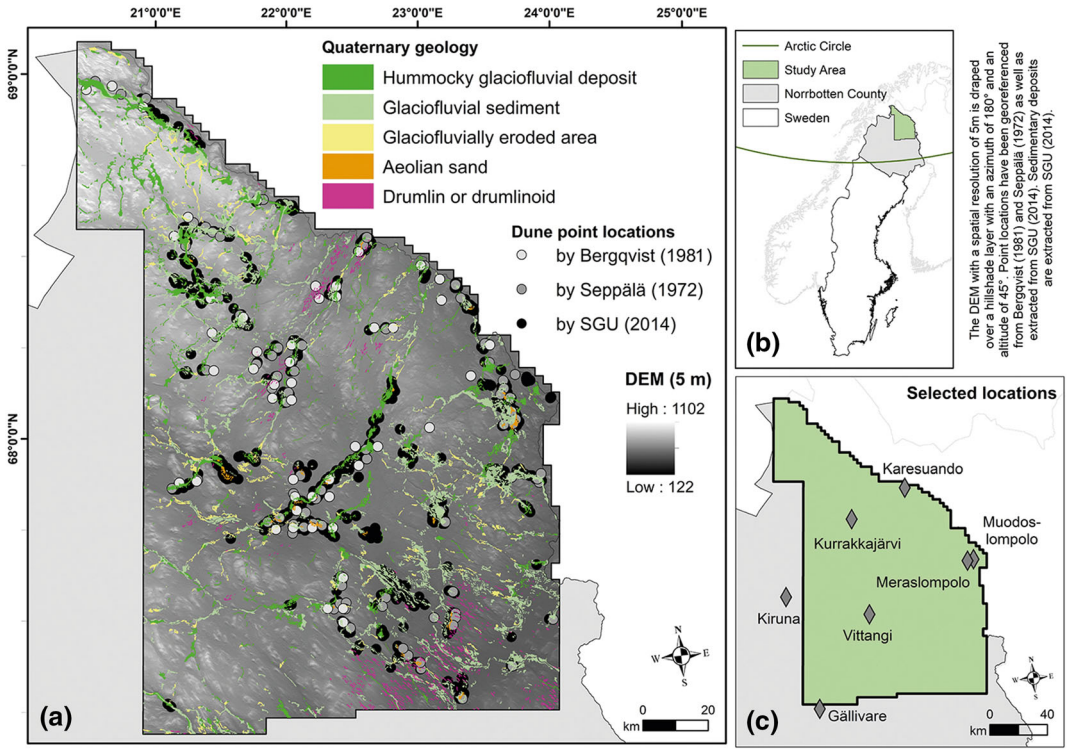

FIGURE 1 Map of the study area located in Arctic Sweden (part of Sápmi) at the borders of Finland and Norway. (a) shows published point data for sand dune locations along with surrounding quaternary geology and a digital elevation model (DEM). The DEM with a spatial resolution of 5 m is draped over a hillshade layer with an azimuth of 180° and an altitude of 45°. Point locations were georeferenced from Bergqvist[23] and Seppälä[4] as well as extracted from SGU.[29] Sedimentary deposits were extracted from SGU.[29] (b) indicates the location of the study area within the Scandinavian Peninsula. (c) locates place names referred to in this study. All data are projected in SWEREF 99 TM [Colour figure can be viewed at wileyonlinelibrary.com]

Assemblages of eskers in north-east Sweden highlight the position of the last remnants of the former ice cover in the northern Scandinavian mountains,[10] and the former presence of ice still impacts the region through a modern isostatic rebound ~10 mm yr^{-1}.[46] Today, Arctic Sweden is characterised by a mean geostrophic wind speed of 8 to 9 m/s and a predominant north-westerly wind direction.[47] Wind speed and direction data from weather stations reveal a prevalence of southerly, northerly and north-westerly winds for Muodoslompolo, as well as strong westerly, south-westerly and southerly winds for Karesuando (see online appendix 1 and 2).

2.1 | Regional dune morphology and dune type

Dunes in Arctic Sweden are predominantly characterised by parabolic shapes,[4,6,19,23] which are typical for their location in a periglacial area.[19,48] Characteristics are U- or V-forms, arms pointing upwind and arms being lower than the main crest[19,28,48] (Figure 2). U- or V-forms are well represented by digital elevation models (DEMs) based on highly resolved light detection and ranging (LiDAR) point data from which the impacts of vegetation cover have been removed[50] (Figure 2a). The windward sides of the dunes are more gentle and contrast with a more pronounced, fine material-dominated lee side.[4,28] Although today's predominant dune shape is parabolic, this may not always have been the case during the early phases of post-glacial dune activity; dominant form today is a function of the emerging form during initial stabilisation and the subsequent effects of reworking events.[28]

The parabolic aeolian sand dunes of Arctic Sweden tend to be located close to sediment sources, such as eskers, glaciofluvial deltas, outwash plains and glacial drainage channels, and are often located in valleys.[4] The presence of Arctic Swedish dunes on former glaciofluvial deltas is less prevalent than further south in Sweden.[23,52] Many of the Arctic Swedish dunes are characterised by parabolas pointing towards the east or south-east, with the parabola arms not exceeding 2 km in length and 15 m in height,[4] here confirmed for non-coalesced systems, for example, near Karesuando (Figure 6d) and the western dunefield near Vittangi (Figure 6a). Only the coalesced system near Kurrakajärvi (Figure 6c) shows greater lengths and heights. Moreover, deflation lakes have often formed in the vicinity of the Arctic dunes, as well as blowouts similar to those described for Arctic Finnish dunes above, indicating dune reactivation and reworking.[23,52] In neighbouring Arctic Finland, stratigraphic evidence of fires and dune reworking suggests a long history of blowout activity during the Holocene.[5,12,14] The precise cause of this reworking is unclear, with some authors evoking natural climate changes,[12] while others suggest that more recent events are anthropogenically forced.[23,53]

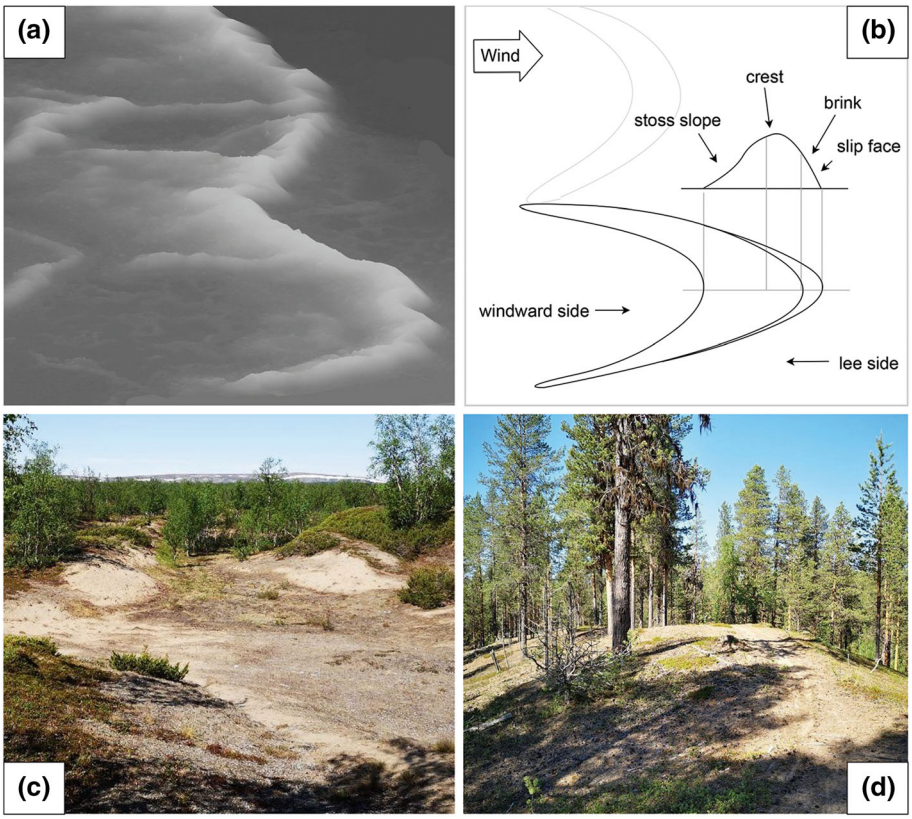

FIGURE 2 Aeolian sand dunes in Arctic Sweden. (a) Coalesced parabolic dunes NW of Karesuando based on light detection and ranging (LiDAR) point cloud (cf. Figure 7d, location 1). 3D mesh was created in CloudCompare based on LiDAR point data by Lantmäteriet.[49] Vegetation was removed using the cloth simulation filter developed by Zhang et al.[50] Note that *z*-scale is 1.5 times the *x*- or *y*- scale. (b) Schematic of the parabolic form based on Yan and Baas.[51] (c) Photograph taken from one main dune crest facing W within a coalesced dune complex west of Lake Kurrakajärvi at 68°16′40.6″N and 21°25'23.0″E on 22 June 2020 by M. Stammler. The dune complex consists of multiple, partially disturbed ridges as perceivable from the photograph. The area is characterised by mountain birch, open sand surfaces, hollows and blowouts, the latter two well shown in this picture. (d) Photograph taken from the dune crest facing NE within a dune complex north of Vittangi at 67°44′32.1″N and 21°38'23.2″E on 21 June 2020. The field of view follows the main dune crest. The area is characterised by pine trees and dry areas that occur in proximity to bogs [Colour figure can be viewed at wileyonlinelibrary.com]

TABLE 1 Data used as a basis for the object-based mapping of sand dunes

	Application	Source	Resolution/ area	Date
GSD – Höjddata, grid 2 + (digital elevation model)	• Elevation data as input to GEOBIA analysis (preprocessed), • derivation of slope and curvature data (unprocessed)	Lantmäteriet	2 m Resampled to 5 m	2009 to 2018 (4,228 tiles)
Orthophotographs, RGB (additional optical data)	• Optical data used for remote checking of results (limited by landforms shadowing and feature shielding due to vegetation)	Lantmäteriet	0.5 m	2016 (132 tiles)
Previous publications with geomorphological maps	• Published point data used as reference for experimental set-up of classification parameters	Seppälä[4]	NE Sweden	Published 1972
		Bergqvist[23]	NE Sweden	Published 1981
Jordarter 1:250,000, nordligaste Sverige (shapefiles with Quarternary geology)	• Geologic and geomorphological information used for interpreting dune polygon location within their geomorphologic setting	SGU	Sweden	Published 2014

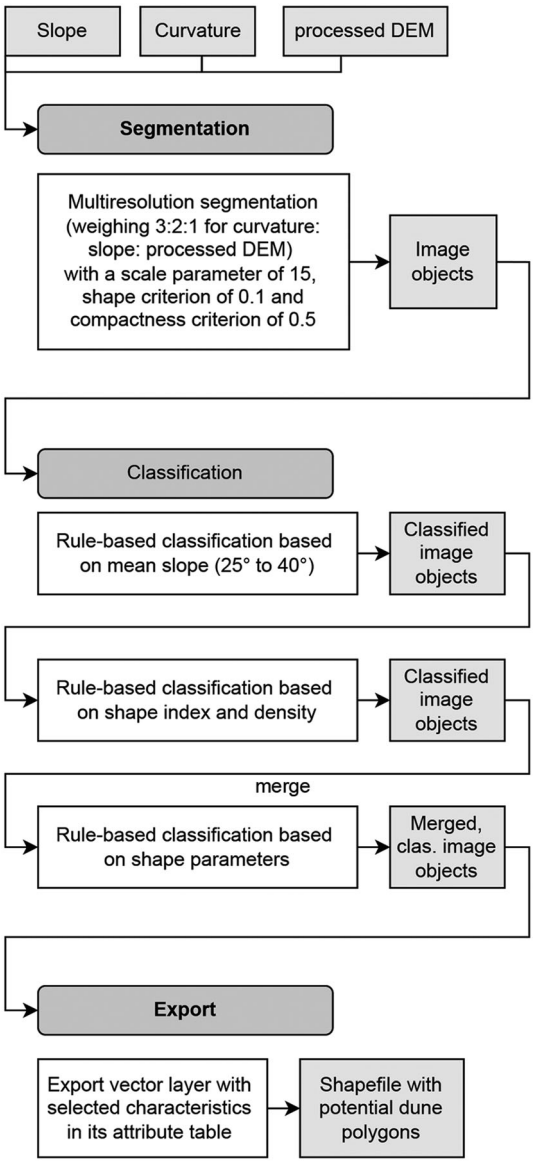

FIGURE 3 Geographic object-based image analysis (GEOBIA) workflow. The workflow can broadly be separated into segmentation, classification and export parts, as visualised by the boxes shown in dark grey. Multiresolution segmentation aims at building image objects based on the homogeneity of selected input parameters [processed digital elevation model (DEM), slope and curvature] within the respective image object. The rule-based classification scheme classifies and refines image objects according to slope and selected shape parameters as well as object size. In the last step, the classified dune objects are exported as shapefiles

3 | MATERIAL AND METHODS

GEOBIA allows meaningful investigation of context within a raster data set while focusing on objects instead of pixels. The approach is rendered possible by high-resolution data where objects of interest are larger than pixels.[39] Software such as eCognition Developer (Trimble Geospatial) can be used to partition remotely sensed data into segmentation-derived image objects. Each object can be semi-automatically classified considering a range of characteristics such as shape and size, texture, information about the context (neighbourhood) of an object, as well as spectral properties. Multiresolution segmentation, which was used in this study, starts with a seed pixel and creates objects that accentuate intra-segment homogeneity and inter-segment heterogeneity, as long as a set of shape and compactness parameters is not exceeded.[37–39,41] This study makes use of the similarities of geomorphic mapping theory and segment-based image classification regarding parameter set-up,[41] with the classification of the segments being rule-based, meaning that a set of characteristics-targeting rules is followed to determine potential aeolian dune sites. Knowledge of and experience in the targeted terrain is essential to this knowledge-based, supervised classification of geomorphological features.[54,55] Working with objects allows for morphology-oriented analysis, whereas pixel-based approaches are limited to spectral information and lead to salt-and-pepper effects, that is, noisy classification results. Object-based results are often considered to be easier to interpret, potentially because GEOBIA mimics human perception.[38,39,56] However, the distinguishability of object-candidates is scale-dependent, a reason why GEOBIA is mainly applied to very high-resolution images.[39]

3.1 | Deriving suitable input data for the GEOBIA analysis

A LiDAR-derived DEM was used as it simulates the surface morphology of the landforms.[44] The 2 m resolution DEM is part of the Ny Nationell Höjdmodell, which is more precisely referred to as 'GSD-Höjddata, grid 2+', and is georeferenced to SWEREF 99 TM and RH 2000,[57] see Table 1. The high-resolution DEM was resampled to 5 m resolution with the aim of decreasing its size and reducing artefacts. This resampled DEM was used to create a residual relief separated DEM following the first stage of residual relief separation, as outlined by Hiller and Smith[27] and originally introduced by Wessel.[58] Returning the median height to a central point was favoured to reduce the strong impact of outliers, which would likely occur when returning a mean value. Furthermore, standard curvature and planar slope data sets were derived from the original, non-resampled DEM. The curvature was unilluminated and, despite amplifying noise,[27] is free from bias.[59] The use of slope values allows for an investigation of the land surface that is not prone to azimuth biasing[59–61] and is independent of other DEM derivatives.[61] The processed DEM and the curvature and slope data sets served as inputs to the geographic object-based image analysis.

3.2 | GEOBIA workflow

The GEOBIA workflow can be divided into segmentation, classification and export stages (Figure 3). First, the multiresolution segmentation algorithm in eCognition Developer 9.5 was used. A weighting of 3 for the standard curvature data set, 2 for planar slope data and 1 for

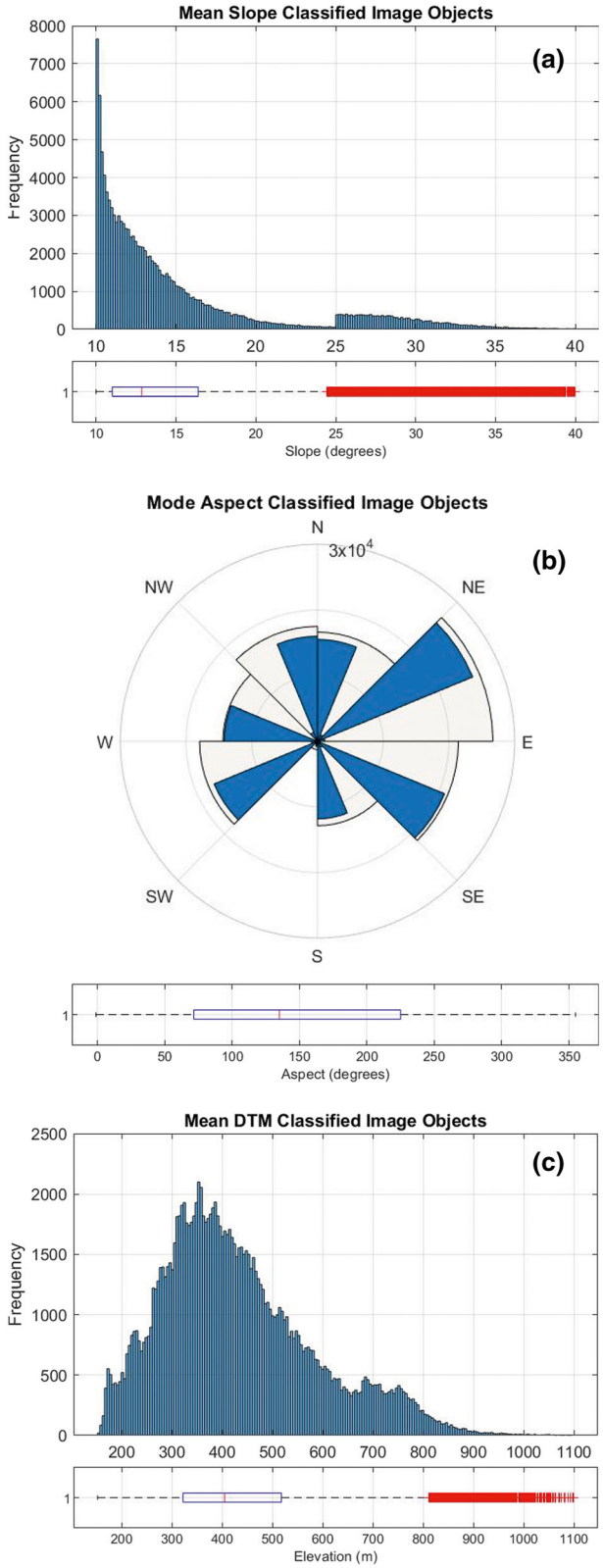

FIGURE 4 Dune characteristics of geographic object-based image analysis (GEOBIA)-classified dune objects for the entire study area. Frequency distributions and boxplots of their (a) mode slope, (b) mode aspect and (c) mode elevation values. The values visualised in red are classified as outliers. Most classified image objects are characterised by a mode slope value of approximately 10° and a mode elevation value of 358 m. A polar histogram (b) reveals a tendency towards the southeast to northeast aspects of dominant slopes. To check whether this is a function of binning category sizes, binning sizes of 16° (blue) and 8° (taupe colour) are shown simultaneously [Colour figure can be viewed at wileyonlinelibrary.com]

the resampled and relief-separated DEM was applied. Parameter set-up was 15 for the scale parameter, along with a composition of the homogeneity criterion of 0.1 for the shape criterion, and 0.5 for the compactness criterion. Multiresolution segmentation is regularly used in geomorphological contexts,[38,41] and its weighting and scale parameter setting is often derived experimentally,[34,38,62] as also for this study. Known point locations for aeolian sand dunes published in the 'Jordarter 1:250 000, nordligaste Sverige' map material[29] and georeferenced from earlier studies[4,19,20,23] allow for an empirical derivation of suitable classification parameter settings, guiding the expert towards potential dune sites or areas where no fieldwork was conducted. The DEM-specific characteristics at these locations, as well as locations known from field reconnaissance, were carefully reviewed. Classification parameters were set based on their suitability for describing the dune sites. We identify upper and lower thresholds of 25° and 40° of slope to best encompass the variability of dune characteristics and apply the functions' shape index, density, area and compactness during classification. The classification workflow first identifies image objects based on their mean slope values. In the second step, image objects that are characterised by shape index and density values that exceed thresholds set in the rule-based classification scheme are excluded. Subsequently, remaining neighbouring image objects are merged to ensure that potentially split dune objects are represented as single objects. Finally, the classified objects are refined by targeting their size and using the software-inherent shape parameters' compactness, density and shape index. The resulting selection of objects obeys all thresholds set during the rule-based classification and is referred to as (GEOBIA/semi-automatically) classified dune objects.

In comparison to using high-resolution optical data for finding dune locations, this approach allows limitations such as feature shielding, where vegetation renders a suitable detection of dunes impossible, to be overcome. Next to classification parameter set-up, published point data were used for a point-to-polygon comparison for validating dune objects at locations where knowledge of dune existence is available based on, e.g., geomorphological maps. Addressing the lack of polygon to polygon comparison due to the unavailability of reference polygon data, dune object extent and shape were assessed during expert decision. Assembling published dune location data from different sources decreases data-inherent subjectivity in geomorphological mapping and feature identification.[63–65]

3.3 | Target-site-related, expert-based acceptance of semi-automatically classified dune objects

Seventeen target sites located within the study area were chosen based on their representativeness for the variety of landscape compositions in the study area, variability in elevation (uplands in the western part of the study area, and flat wetland in the eastern part), in latitude (67.7° to 68.5°), and in vegetation cover (open tundra landscape to pine forest). Areal sizes of the target sites range between 8 and 138 km^2 and amount to 615 km^2 in total, thus representing 3% of the entire study area. The decision over target sites is expert-based and relies on field reconnaissance, the LiDAR-based high-resolution DEM, high-resolution optical data and the SGU[29] data set on landforms and Quaternary geology. At these sites, the GEOBIA-classified dune objects were manually evaluated for true-and-false positives based on expert knowledge. Similarly, areas without classified dunes were checked at selected sites within the target areas to avoid missing dunes in the classification. Expert-based decision on GEOBIA-classified dunes was aided by the use of several z-factor-exaggerated and non-exaggerated hillshades derived from the original DEM, as well as the planar slope data set. The final selection of dune polygons consisted of GEOBIA-classified dune objects that were expert-accepted and are referred to as expert-accepted dune objects. Point to polygon comparison between published point data (1:250,000) and classified dune objects derived from a 5-m resolved DEM likely suffers deviation caused by differences in resolution, which is unavoidable due to the scarcity of published validation data.

4 | RESULTS

4.1 | Slope, aspect and elevation characteristics of GEOBIA-classified dune objects

Semi-automatically classified dune objects are available for the entire study area, thus, allowing for a large-scale analysis of their characteristics. Figure 4 shows the results of the area-wide analysis of all semi-automatically classified dune objects' slope, aspect and elevation values. Slope value input to the GEOBIA analysis is based on the 2-m non-relief-separated DEM and extracted as the respective mode value of each object semi-automatically classified as dune. Aspect data are based on the slope value input data set, and elevation data are retrieved from the preprocessed DEM. While object mode values indicate the most frequently occurring value of the object, object mean values are affected by outliers and likely underestimate the dominant slopes due to the occurrence of zero/near zero slopes on the top of sand dunes. Due to their insensitivity to outliers, modal values were investigated for dune slopes, the aspect of dominant slopes and elevation data. Mode slope values of the GEOBIA-classified dune objects are characterised by a stark maximum in frequency occurring at 10.3°.

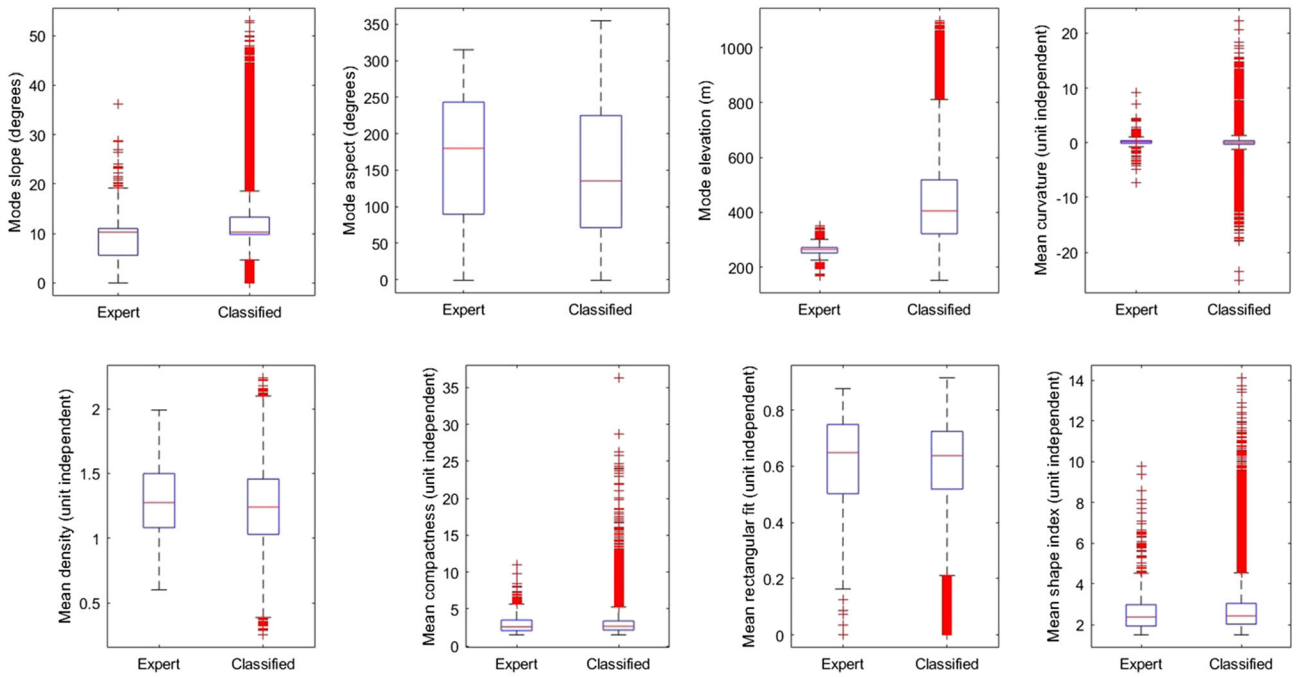

FIGURE 5 Comparison of key image object characteristics for expert-accepted image objects ($n = 517$) and for all the geographic object-based image analysis (GEOBIA)-classified dune objects ($n = 128{,}726$) based on mode slope, aspect and elevation, and mean curvature, density, compactness, rectangular fit and shape index values. Boxplots provide insight into the suitability of the parameter selection. The values visualised in red are classified as outliers [Colour figure can be viewed at wileyonlinelibrary.com]

Mode aspect values show a tendency towards the east and south-east (cf. online appendix 3). The majority (mode) of the semi-automatically classified dune objects in the study area occur at an elevation of approximately 358 m, with a median of 405 m.

4.2 | Comparison of GEOBIA-classified and expert-accepted dune objects

Figure 5 compares the statistical characteristics of the expert-accepted and semi-automatically classified dune objects. The mode slope, aspect and elevation characteristics of the semi-automatically classified dune objects are compared to the mode slope, aspect and elevation characteristics of the classified and later expert-accepted dune objects that are available for the 17 selected target sites. Curvature and shape characteristics were investigated using mean values to accommodate the range of values possible within one polygon, as well as to take into account the entire range of values in terms of shape characteristics. The expert-accepted and semi-automatically classified dune objects display a strong similarity in the median of modal slope values and width of range. The range and location of the interquartal range (IQR) of the mode aspect values are also similar and broadly agree with observed dune orientation, although the interpretation of dune aspect values may be ambiguous due to multiple slope aspects in individual dunes. Mode elevation values show strong differences in IQR, indicating limited representativeness of the expert-sampling in terms of altitude. Mean curvature distributions are characterised by a symmetrical pattern above and below the distribution median. Furthermore, all shape characteristics calculated from functions available in eCognition Developer 9.5 are characterised by strong coherence in the comparison between classified and expert-accepted, as well as solely semi-automatically classified image objects.

Figure 6 shows the semi-automatically classified dune objects, as well as the classified and expert-accepted dune objects for the target sites near Vittangi, Meraslompolo, Kurrakajärvi and Karesuando. The mapped polygons are shown together with published point data for dune locations. Both the point and polygon data sets are coherent in general location, with the polygons comprising additional information on the exact location of the landforms, as well as the shape and orientation of the mapped features. The results show that the polygons are

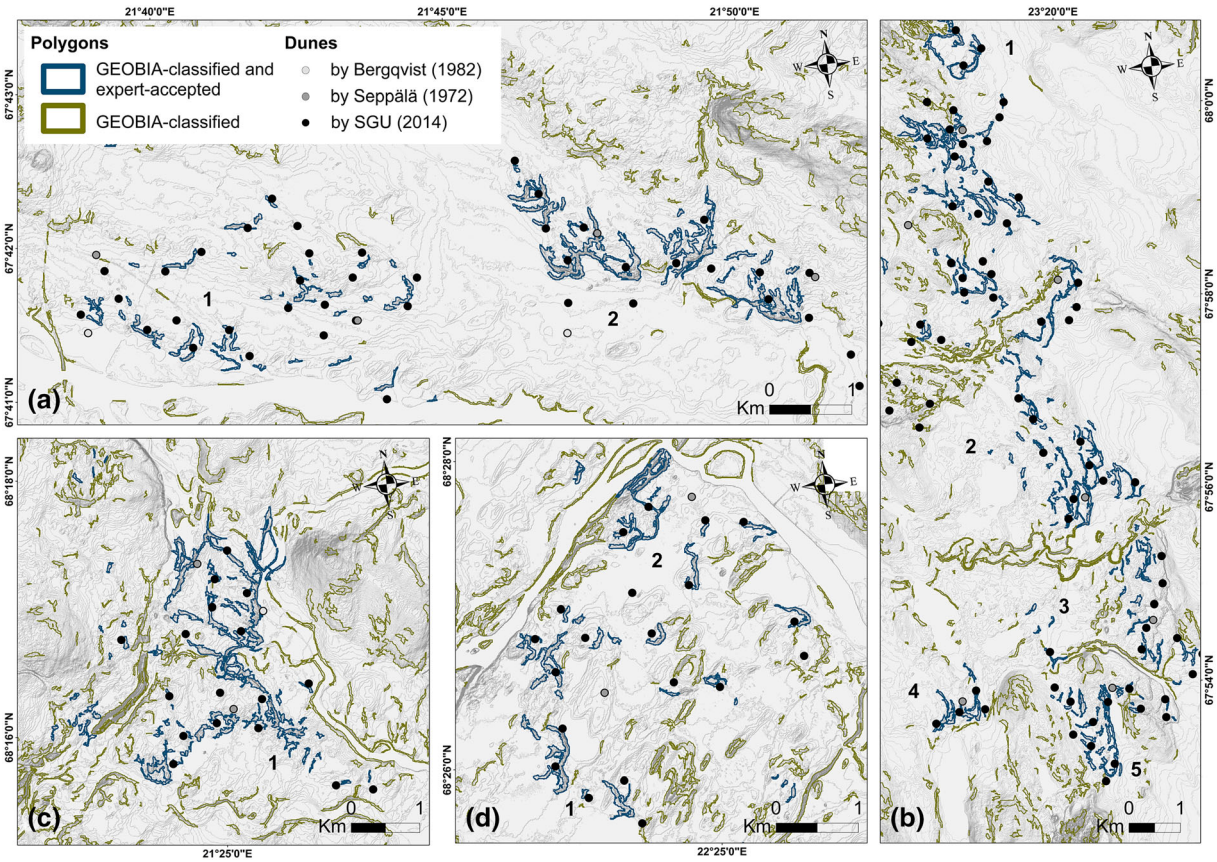

FIGURE 6 Classified and expert-accepted sand dune sites located (a) NE of Vittangi, (b) west of Meraslompolo, (c) west of Kurrakkajärvi and (d) around Karesuando, shown together with point data for dune locations georeferenced from Bergqvist,[23] Seppälä,[4] and extracted from SGU.[29] All classified image objects are visualised in green; dark-blue polygons remain after expert decision. Numbering refers to locations described in the text, as well as shown in Figure 7. White space in the upper-right corner of (d) is due to lack of data for Finland (river constitutes the Swedish-Finnish border). Point and polygon data are visualised on two hillshades (azimuth 135° and 315°, altitude 45°) to minimise azimuth biasing. All data are projected in SWEREF 99 TM [Colour figure can be viewed at wileyonlinelibrary.com]

predominantly c-shaped (e.g. Figure 6b, location 2) and that single polygons occur next to coalesced polygons (e.g. Figure 6a, locations 1 and 2). Displaying the results in a map further shows that polygons that are highly pronounced and well developed in their shape occur next to less-pronounced polygons (Figure 6a, locations 1 and 2). Figure 6 also indicates that a similar orientation of c-shapes in the study area is prevalent, with minor differences in polygon orientations being possible in close proximity (Figure 6b, locations 3 and 5). The findings near Vittangi, Meraslompolo, Kurrakajärvi and Karesuando are confirmed by the results based on the remaining target sites (cf. online appendix 4).

5 | DISCUSSION

5.1 | Segmentation and classification process

Applying GEOBIA reduces the effort required for time-consuming and expensive field mapping.[66] Furthermore, GEOBIA inherent algorithms produce transparent, consistent and reproducible results, thus reducing human bias.[60,65] Nonetheless, the observer's influence when accepting results needs to be acknowledged,[39,65] as well as the dilemma between ensuring quality and increasing subjectivity inherent when introducing expert decisions in the workflow.[41,54,55] While acknowledging these uncertainties, we infer that the expert-control increases the quality of results based on comparing the mapping results at the target sites (cf. Figure 6, online appendix 4). It delivers a controlled means of insight into the suitability of the segmentation and classification process based on a comparison of object characteristics (cf. Figure 5). Through the sole use of a DEM and its derivatives, planar slope and standard curvature, and by abstaining from the use of optical data to segment aeolian sand dunes in Arctic Sweden, this study eliminates landform shadowing[67] and feature shielding due to vegetation.[4] Further, this choice reduces computing time and processing power. The sole use of a DEM is facilitated by dune slope characteristics that strongly differ from the landform surroundings, such that slope represents an excellent indicator of dune landform existence. Ruleset transferability allows for increasing the spatial scale without introducing inter-coder variability,[68] which permits intensive mapping of areas that would be difficult to undertake by means of expert-based manual mapping. However, we expect that implementing fixed thresholds in the knowledge- and rule-based classification with

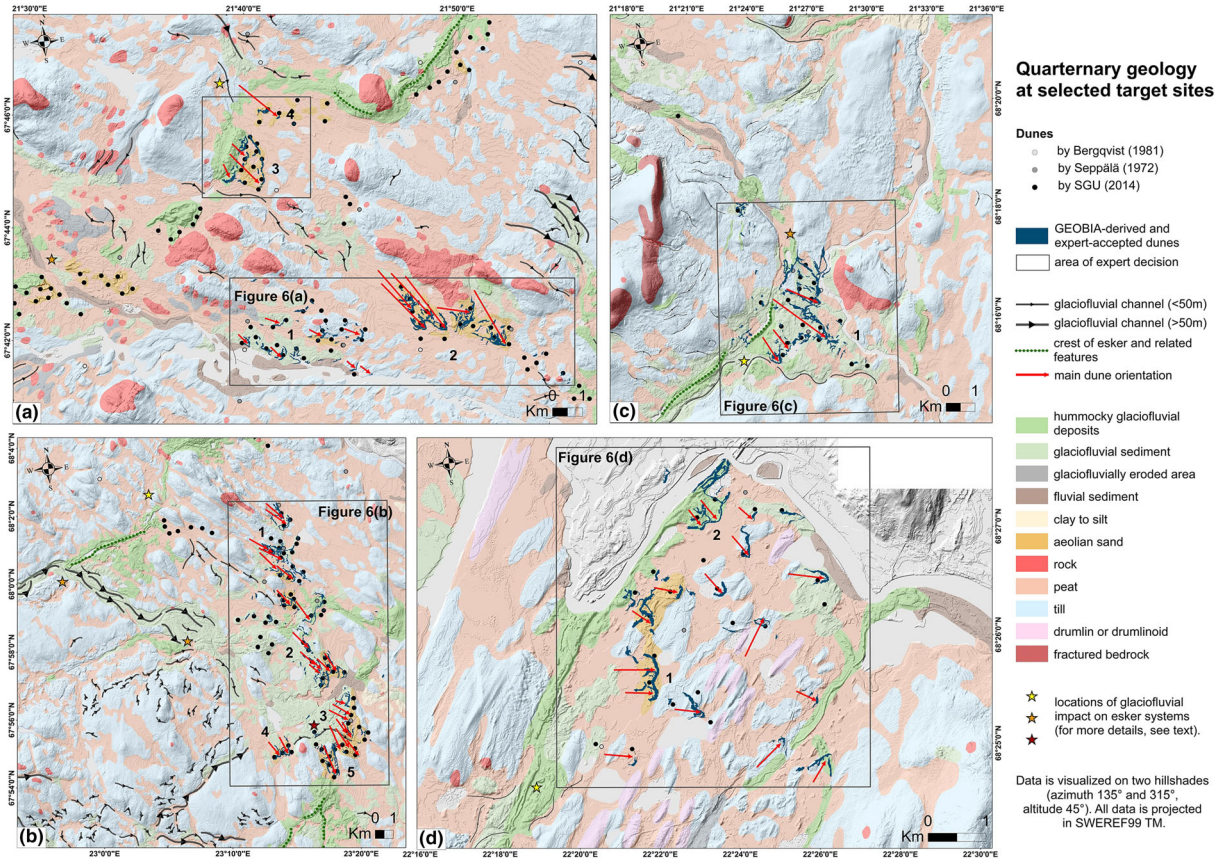

FIGURE 7 Maps of the quaternary geology and geomorphology in the surroundings of (a) Vittangi, (b) Meraslompolo, (c) Kurrakkajärvi and (d) Karesuando, including the geographic object-based image analysis (GEOBIA)-derived and expert-accepted dune locations for the dune complexes. Grey dashed lines represent target site extent as shown in Figure 6 and thus the limit of expert decision. Length of arrows changes in approximation to dune size. Point data georeferenced from Bergqvist[23] and Seppälä,[4] all other data published by SGU[29] in the data set 'Jordarter 1:250 000, nordligaste Sverige'. The data are projected in SWEREF 99 TM [Colour figure can be viewed at wileyonlinelibrary.com]

empirically derived parameters as used in this study is one of the main drivers of false positives (dune polygons at target sites that are semi-automatically classified but not expert-accepted; e.g. meandering river banks, cf. Figure 6). On the contrary, upper and lower boundaries of fixed thresholds can also lead to the removal of features that should have been classified but only slightly miss the selected threshold(s). We estimate a high degree of completeness due to the possibilities of checking the correct mapping of dune sites known from field reconnaissance, and from the comparison of our mapping results to the previously mapped dune sites. We allow larger systems to be split during segmentation to avoid dismissing small features and merge complex and potentially split systems during the classification process of the GEOBIA analysis. Completeness can be confirmed only for dunes which comply with the parameter set-up, as these are the dunes targeted by the classification ruleset. Dunes which do not comply with the parameter set-up were missed (true negatives).

Expert-based selection of classification thresholds can be avoided by using machine learning approaches,[69,70] as exemplified for the classification of aeolian landforms by Fitzsimmons et al.[34] However, limited objectivity must also be acknowledged for machine learning due to expert-chosen training sites, potential uncertainty inherent to the training data (e.g.[71]) and manually set parameters (e.g.[72]). We suggest that the expert-checked data sets of the 17 target sites represent valuable validation data for future studies that apply machine learning approaches to mapping aeolian sand dunes in Arctic Sweden.

Published point data are generally located in close proximity to the classified dune objects. However, the precise location of points and polygons predominantly matches only in the case of dune ridges characterised by high slopes between the dune crest and surrounding landscape, here referred to as pronounced dune ridges (Figures 6 and 7, cf. online appendix 4). For example, point locations and highly pronounced dune ridges at the Vittangi site fit closely (Figure 6a, location 2), whereas point data are located several 10s of meters away from the less-pronounced dune ridges (Figure 6a, location 1). Similarly, a very pronounced ridge in the Karesuando dune field (Figure 6a, location 1; also Figure 2a) is characterised by closely corresponding point and polygon data, while several points are located at a similar distance to single dune polygons as in the example of Vittangi above (Figure 6c, location 3). Furthermore, up to 10% of point locations do not correspond with dune objects at all and are confirmed to be true negatives (e.g. Figure 6a, location 2, south of the coalesced system), while some dune objects have not been previously mapped as point data (e.g. Figure 6c, location 1).

As the classified dune objects are based on geomorphometric characteristics of aeolian sand dunes, we infer that the semi-automatic mapping, together with the expert-decision, leads to a more reliable and precise detection of the landform, especially if the form is weakly pronounced. By including dune areal information as polygon data, the analysis further allows accurate interpretation of the occurrence of large coalesced dune systems, whereas point data cannot include information on coalescence. This greater accuracy and spatial coverage, along with the detection of objects missed in traditional mapping, allows for a better representation of the true dune coverage in an area and a more accurate interpretation of the causes of dune formation in relation to other landforms.

5.2 | Geomorphological interpretation of the expert-accepted dune objects

The GEOBIA-derived dune sites near Vittangi, Meraslompolo, Kurrakajärvi and Karesuando are mapped alongside selected Quaternary geology to understand their landscape associations and the reasons behind dune characteristics (Figure 7). Importantly, such interpretations would not be possible without mapping these dunes as objects, as point data cannot convey, e.g., morphology. Besides the benefits, challenges in dune object analysis occur due to natural landform variability and the impact on, e.g., mode slope and mode aspect. We hypothesise that main dune nose slipfaces are dominant in the mapped polygons as their slope values were targeted during GEOBIA analysis and each object's most dominant value (mode) was extracted. Despite this representation of dune nose slipfaces, the mode aspect derived from these slope values can offer partial help only in determining the true orientation of parabolic sand dunes in the study area. In addition to dune nose slipfaces, dune arm slipfaces impact the mode aspect data set (arm strike) and, therefore, the calculated mode aspect direction. This highlights the need for additional geomorphological interpretation of dune objects and a morphology-based determination of dune orientation.

The interpretation of mapped aeolian sand dunes is based on the expert-accepted selection of classified dune objects. Investigating these expert-accepted dune locations confirms an abundance of dunes of parabolic type, as anticipated from the existing literature.[4,6,19,23] The dunes occur as single dunes as well as coalesced systems at the Vittangi, Meraslompolo and Kurrakajärvi sites (Figure 7a–c), with their shapes being pronounced to different degrees, e.g., at the Vittangi site (Figure 7a). The mode slope values of 10.3° for the expert-accepted as well as for the classified dune polygons strongly correlate with the lower end of values in the literature for windward sides of parabolic Arctic Swedish aeolian dunes.[4] The dominant elevation (mode) of 358 m for the semi-automatically classified dune objects lies close to the modern limit of pine (*Pinus sylvestris*) forest or forest stands, and indicates that considerable numbers of dunes must also exist in the birch forest and tundra zones.

5.2.1 | Wind directions inferred from dune polygons

The mapped Arctic Swedish aeolian sand dunes show a tendency to a south-east orientation, partially supported by prevalent dune object mode aspect values (cf. Figures 4b, 6, 7, and online appendix 3). As the inner, stoss side of a dune parabola faces the dominant wind responsible for sand drift,[18,19] sand transporting winds during dune stabilisation (and reactivation) likely had a dominantly north-westerly component (Figure 7, red arrows). The meteorological station in

Muodoslompolo is located approximately 5 km east of the Meraslopolo dune fields (Figure 7b) and was operated from 1965 to 1996. Analysis of the measured wind data split at both 8 and 6 m/s, thresholds inspired by Barchyn and Hugenholtz et al.[30] and determined experimentally, reveals that winds with speeds above 6 m/s but below 8 m/s are disproportionately represented by northerly and north-westerly winds during the generally snow-free months of May and June (cf. online appendix 1). May and June are specifically important for dune movement due to predominantly warmer temperatures, lower soil moisture and therefore decreased cohesion. January and March are characterised by southerly winds which cannot be related to the dune orientations as mapped here, suggesting sheltering effects of snow cover on potential sand sources, as discussed in Koster[6] and Seppälä,[19] or that frozen ground during the winter months would have prevented sand movement.

Aeolian sand dunes near Karesuando are characterised by a variability of east-south-east to south–south-east facing dunes (Figure 7d). Recent wind directions measured at the weather station in Karesuando, which was operated from 1939 to 2011 (cf. online appendix 2), indicate a prevalence of westerly and southerly winds for wind speeds above 6 m/s and below 8 m/s. Westerly winds are exclusively dominant in May and June, whereas southerly winds dominate over westerly winds in January and November. Deflation during the drier summer months characterised by less cohesion and no snow sheltering, similar to the situation near Muodoslompolo, is thus very likely and is supported by the dune orientation at the Karesuando dune site. While the seasonality of local wind patterns along with the climate's impact on cohesion and vegetation highlights the sensitivity of the aeolian landform towards changes in climate, the similarity of dune orientations to current wind directions during spring and early summer implies a relative constancy of wind dynamics over the Holocene since the initial dune stabilisation.

5.2.2 | Topographic control inferred from dune polygons

Aeolian sand dunes in Arctic Sweden appear to be topographically controlled in many instances, with topography playing an important role in diverting winds, thus impacting dune type, location and orientation. At the Vittangi site (Figure 7a), north-westerly winds during the formation/stabilisation of the dunes most likely travelled around the topographic obstacles that are located north-west of locations 1 and 3 and have thereby potentially caused the deviation in orientation of the south-easterly pointing dunes at location 1, in comparison to the south-south-easterly pointing dunes at location 2. At the Meraslompolo site (Figure 7b, location 1), the drumlinisation of till that Hättestrand et al.[45] classified as part of a relict glacial landscape creates valleys aligning north-west to south-east. The dunes in this area are also oriented with the parabola facing south-east, suggesting that these valleys act to funnel the wind, potentially increasing the transport capacity of the airflow.[76]

The dune complex near Kurrakajärvi (Figure 7c) is located so that winds driving its formation must have travelled around the fractured bedrock west of the dune complex, resulting in esker erosion, sediment transport and sand deposition. Importantly, this dune field formed behind a local topographic obstacle while sand supply is present along the south-west to north-east expanding esker system. Due to the large size of the dune complex, it appears that the wind transport capacity must have been high and/or consistent over a longer time period during dune formation to be able to transport the volume of sand deposited. Hesp and Smyth[73] highlight that airflow around a curved object causes marginal and downwind bed erosion, with vortices originating from wind deflection by the obstacle leading to a local increase in transport capacity to an obstacle's lee.[74] With respect to the dune field west of Kurrakajärvi, we hypothesise that the existence of fractured bedrock outcrop has likely contributed to dune formation as it locally increased wind speeds, thereby enabling transportation of sediment away from the esker. This mode of dune formation contrasts with the mechanism proposed from obstacles slowing down winds, thus forcing dune formation by decreasing wind transport capacity.[19,28] Acknowledging that parabolic dune orientation is a product of climatological as well as topographic factors, we infer that topographic obstacles play a major role in controlling sediment transporting winds in Arctic Sweden and that local topography has a major impact on dune orientation and position.

5.2.3 | Sediment routing inferred from dune polygons

Sediment supply control is a crucial factor for cold-climate sand dune formation, specifically with regard to dune size.[77,19] Climatic and topographic control on sand availability leads to different locations where sand is stored. Geomorphic associations visualised based on the new mapping (Figure 7) show that esker systems act as dominant sediment sources, as perceivable from the green shading on the polygon-deduced upwind side (Figure 7, red arrows) of the dune systems near Vittangi, Meraslompolo, Kurrakajärvi and Karesuando. This confirms general suggestions of dune proximity to eskers and glaciofluvial deltas in Fennoscandia[4] and reveals the locations of aeolian sand dunes downwind of disturbed esker systems at all four target sites. In addition, the mapping reveals that esker systems at locations where glaciofluvial and fluvial activity has disturbed the esker are especially significant (Figure 7, yellow to red stars).

At the Vittangi site (Figure 7a), sediment availability for dune formation at location 2 was likely controlled by glaciofluvial activity at the location indicated by the yellow star, and controlled by fluvial disturbance (fluvial sediment, brown) of the esker system (green) at the orange star for location 1. At the Meraslompolo site (Figure 7b), glaciofluvial sediments upwind of the dune location likely contributed to dune formation. In addition, we infer that glaciofluvial activity played a role in activating sediments for location 1 from eskers at the yellow star, at the orange stars with respect to locations 2 and 4 and at the red star for locations 3 and 5. The pattern of sand availability upwind of dune locations coinciding with (glacio)fluvial meltwater activity is further showcased at the Kurrakajärvi and Karesuando sites

(Figure 7c,d). For example, the patchy occurrence of glaciofluvial sediments along Kenttäkoski River east of the dune site near Kurrakajärvi (Figure 7c) and the direction of the esker are suggestive that before (glacio)fluvial impact the esker extended north-east. In addition, glaciofluvial sediments just upwind of the dune locations certainly contributed material for formation. We infer that the main activation of source material occurred due to glaciofluvial (and/or fluvial) interaction with the esker system (cf. Figure 7). Thus, mapping the dune polygons together with the surrounding Quaternary geology demonstrates the (glacio)fluvial control of geomorphic and sedimentary systems on sand availability for dune formation in Arctic Sweden.

After initial deposition, larger parabolic dunes appear to represent a sediment source to secondary dunes located downwind, e.g., in the case of multiple coalesced arcs of dunes and single dunes located east of the nose of the major Kurrakajärvi dune system (Figure 7c, location 1). Based on signs of recent erosion of the Kurrakajärvi complex perceived in the field (cf. Figure 2c), as well as reported for aeolian sand dunes in Arctic Sweden by Bergqvist,[23] we hypothesise that the depositional landforms act as sediment sources once reactivated, rather than downwind dunes being deposited earlier than the main complex. We suggest direct dating to clarify the secondary status of the dunes by determining their age in relation to the main dune complex.

5.2.4 | Timing of dune stabilisation inferred from dune polygons

With dune type being the result of multiple factors,[28] the timing of dune stabilisation can, to some extent, be interpreted based on the dominance of parabolic dune type inferred from object-based image analysis. Parabolic dune formation is related to the existence of vegetation cover that decreases the wind's transport capacity.[19,28] Post-glacial pine invasion into Arctic Finland occurred approximately 9,000 years ago,[15] which might suggest initial dune stabilisation and the formation of incipient parabolic forms at a similar time over Arctic Sweden, and consequently in this study area. However, parabolic dunes in the Finnish Arctic are known to have been reworked over multiple phases,[12,17] and given the existence of blowouts in current dune areas of Arctic Sweden (Figure 2c), this reworking also seems likely to have occurred for dunes in this region. As such, it is unclear to what extent today's parabolic forms are a relic of the initial stabilisation, or rather the progressive reworking and enlargement of the parabolas with periodic reworking in the Holocene.

The mapping here shows that sequences of coalesced dunes occur in the dune fields near Vittangi, Meraslompolo and Kurrakajärvi (Figure 7a, location 2; Figure 7b, location 5, 7c). These multiple ridge systems may indicate that multiple dune-forming episodes have occurred, with successive ridge systems developing over the Holocene since initial sand movement, or rather that the multiple separated ridges were active simultaneously, as shown, e.g., in SW France[75]; these possibilities can only be tested via direct dating.

While dunes are connected to or located in close proximity to esker systems at all four target sites (Figure 7a, location 1; Figure 7b, location 2; Figure 7c,d, location 2), more distantly located dunes (Figure 7a, location 2 and Figure 7d, location 1) can also be identified. Increased distance to dune sediment sources probably indicates more extensive periods of mobility or multiple phases of reactivation and reworking. Very well-developed dunes next to less extensive dunes near Vittangi (Figure 7a, locations 1 and 2) can either be a result of the combined impact of sand availability and wind transport capacity and/or indicate deposition of these forms at different points in time. We infer that reduced sand availability, wind capacity and/or depositional processes occurring over shorter timescales lead to less material being transported away from the esker system, thus, producing less-pronounced dunes for location 1. In contrast, the extensive dunes in location 2 suggest rather high sand availability, together with strong wind capacity and/or deposition over a longer timescale. Thus, the differences in the occurrence of dune shapes are inferred to be a product of process rates or timescales. Our mapping, therefore, provides the opportunity for a detailed reconstruction of post-glacial landscape evolution, in combination with direct dating of landforms.

6 | CONCLUSIONS

Systematic spatial analysis of Arctic Swedish aeolian sand dunes using GEOBIA allows for reproducible mapping on a larger scale, combining expert knowledge and semi-automation. This demonstrates that expert control, an essential characteristic of traditional geomorphological mapping, and the use of innovative and machine-based approaches such as GEOBIA are not mutually exclusive. As such, combining these complementary approaches contributes to a more robust outcome. Semi-automated detection as well as ruleset transferability allow for an increase of the spatial scale in a computationally non-extensive manner, while expert decision ensures the quality and suitability of the segmentation and classification process.

This large-scale analysis resulted in a higher number of mapped dunes than before, and more precise mapping and form analysis of these overwhelmingly parabolic dunes. Furthermore, the approach more reliably detects less-pronounced aeolian sand dunes in the study area and prevents misinterpretation of, e.g., coalesced systems, as erroneous counting of multiple single ridges instead of a coalesced system can be prevented by determining the landform boundaries. The widespread presence of the parabolic dune type, as suggested by previous traditional dune mapping in Arctic Sweden, is confirmed. Expert-accepted dune objects are characterised by slope values which are similar to lower-end literature-based values for the windward sides of Arctic Swedish aeolian sand dunes. Many dunes are oriented with noses facing south-east, thus indicating a dominant north-westerly sand transporting wind direction during formation and reworking. The orientation appears in many instances to be topographically controlled, and the similarity of the orientation direction to current wind directions during spring and early summer implies a relative constancy of sand transporting wind dynamics over the Holocene since initial dune stabilisation.

Geomorphic associations, visualised based on the new mapping, show that esker systems act as dominant sediment sources, with the

potential for major dunes and dune complexes acting as sediment sources to secondary smaller dunes, once reactivated. Glaciofluvial and fluvial forcing of sand availability appears likely in all studied cases, either directly or indirectly via disturbance of esker systems, and implies that initial dune formation is strongly linked to landscape processes during and immediately after deglaciation. However, to what extent these dunes are reworked during the Holocene remains unclear. The detailed mapping presented here provides a framework for which this can be tested, e.g., via a coupled analysis of the spatial associations of multiple dune ridges with respect to sediment sources and information derived from direct age dating of dune movement and stability. The results of this study on the timing of dune stabilisation further highlight the need to investigate Arctic Swedish aeolian sand dunes as objects to understand local and regional landscape associations and evolution. Such large-scale analysis can help decode past landscape (in)stability and frame understanding of potential future changes in an area that already today is outpacing predictions of global climate change impact.

ACKNOWLEDGEMENTS

This research was funded by the Göran Gustafsson Foundation (grant no: 1929) to T.S. M.S. is thankful for Trimble eCognition which generously supported this study by sponsoring an eCognition Developer 9.5 license. The authors thank Rickard Pettersson (Uppsala University), Veijo Pohjola (Uppsala University), Ramona Schneider (Uppsala University), Salome Oehler (Stockholm University) and Simon König (Bavarian Forest National Park Administration) for helpful discussions. M.S., T.S. and D.H. declare that they have no conflicts of interest. Open Access funding enabled and organized by Projekt DEAL.

DATA AVAILABILITY STATEMENT

The data that support the findings of this study are available from the corresponding author upon request.

ORCID

Melanie Stammler https://orcid.org/0000-0002-9626-7548
Thomas Stevens https://orcid.org/0000-0002-6662-6650
Daniel Hölbling https://orcid.org/0000-0001-9282-8072

REFERENCES

1. IPCC. Summary for policymakers. *Clim Change Impacts, Adapt Vulnerability - Contrib Work gr II to Fifth Assess Rep*. 2014;35(7):1-32. doi:10.1016/j.renene.2009.11.012
2. Hanssen-Bauer I, Førland EJ, Hisdal H, Mayer S, Sandø AB, Sorteberg A. (2019). Climate in Svalbard 2100 - a knowledge base for climate adaptation.
3. Overland J, Dunlea E, Box JE, et al. The urgency of Arctic change. *Pol Sci*. 2019;21:6-13. doi:10.1016/j.polar.2018.11.008
4. Seppälä M. Location, morphology and orientation of inland dunes in northern Sweden. *Geogr Ann Ser B*. 1972;54(2):85-104. doi:10.1080/04353676.1972.11879860
5. Käyhkö JA, Worsley P, Pye K, Clarke ML. A revised chronology for aeolian activity in subarctic Fennoscandia during the Holocene. *Holocene*. 1999;9(2):195-205. doi:10.1191/095968399668228352
6. Koster EA. Ancient and modern cold-climate aeolian sand deposition: a review. *J Quat Sci*. 1988;3(1):69-83. doi:10.1002/jqs.3390030109
7. Wolfe SA. *High latitudes*. 2nd ed. Encyclopedia of Quaternary Science: Second Edition. Elsevier B.V; 2013. doi:10.1016/B978-0-444-53643-3.00152-7.
8. Alexanderson H, Bernhardson M. Late glacial and Holocene sand drift in northern Götaland and Värmland, Sweden: sediments and ages. *GFF*. 2019;141(2):84-105. doi:10.1080/11035897.2019.1582559
9. Lundqvist J, Mejdahl V. Luminescence dating of the deglaciation in northern Sweden. *Science*. 1995;28:193-197. doi:10.1016/1040-6182(95)00031-D
10. Stroeven AP, Hättestrand C, Kleman J, et al. Deglaciation of Fennoscandia. *Quat Sci Rev*. 2016;147:91-121. doi:10.1016/j.quascirev.2015.09.016
11. Clarke ML, Käyhkö JA. Evidence of holocene aeolian activity in sand dunes from Lapland. *Quat Sci Rev*. 1997;16(3-5):341-348. doi:10.1016/S0277-3791(96)00109-6
12. Matthews JA, Seppälä M. Holocene environmental change in subarctic aeolian dune fields: the chronology of sand dune re-activation events in relation to forest fires, palaeosol development and climatic variations in Finnish Lapland. *Holocene*. 2014;24(2):149-164. doi:10.1177/0959683613515733
13. Seppälä M. Deflation and redeposition of sand dunes in finnish Lapland. *Quat Sci Rev*. 1995;14(7-8):799-809. doi:10.1016/0277-3791(95)00057-7
14. Van Vliet-Lanoe B, Seppala M, Kayhko J. Dune dynamics and cryoturbation features controlled by Holocene water level change, Hietatievat. *Finnish Lapland Geol en Mijnb*. 1993;72:211-224.
15. Kultti S, Mikkola K, Virtanen T, Timonen M, Eronen M. Past changes in the scots pine forest line and climate in Finnish Lapland: a study based on megafossils, lake sediments, and GIS-based vegetation and climate data. *Holocene*. 2006;16(3):381-391. doi:10.1191/0959683606hl934rp
16. Nota K, Klaminder J, Milesi P, et al. Norway spruce postglacial recolonization of Fennoscandia. *Nat Commun*. 2022;13(1):1-9.
17. Käyhkö J, Pye K, Worsley P. Quantitative mapping of active aeolian surfaces in northern Fennoscandia - Landsat TM hybrid classification. *Eur Sp Agency, Spec Publ*. 1996;391:147-152.
18. Ahlbrandt TS, Fryberger SG. *Eolian deposits in the Nebraska Sand Hills*. US Geol. Surv. Prof. Pap; 1980:1120.
19. Seppälä M. *Wind as a geomorphic agent in cold climates*. Cambridge University Press; 2004.
20. Högbom I. Ancient inland dunes of northern and middle Europe. *Wiley Behalf Swedish Soc Anthropol Geogr*. 1923;5:113-243. doi:10.2307/519659
21. Högbom I. Finiglaziale Flugsandfelder in Dalarne. *Geol Föreningen I Stock Förhandlingar*. 1913;35(7):484-500. doi:10.1080/11035891309446986
22. Hörner N. Brattforsheden: ett värmländskt randdeltekomplex och dess dyner. SGU Avh. och Uppsats. Serie C. 1927.
23. Bergqvist E. *Svenska inlandsdyner: översikt och förslag till dynreservat*. Uppsala; 1981.
24. Bergqvist E, Lindström E. Bevis på subrecent eolisk aktivitet på Brattforshedens inlandsdyner. *Geol Föreningen I Stock Förhandlingar*. 1971;93(4):782-785. doi:10.1080/11035897109451550
25. Alexanderson H, Bernhardson M, Kalinska-Nartisa E. Aeolian activity in Sweden: An unexplored environmental archive, LUNDQUA Report. 2016.
26. Bernhardson M, Alexanderson H. Early Holocene dune field development in Dalarna, Central Sweden: a geomorphological and geophysical case study. *Earth Surf Process Landf*. 2017;42(12):1847-1859. doi:10.1002/esp.4141
27. Hiller JK, Smith M. Residual relief separation: digital elevation model enhancement for geomorphological mapping. *Earth Surf Process Landf*. 2008;33(14):2266-2276. doi:10.1002/esp.1659

28. Pye K, Tsoar H. *Aeolian sand and sand dunes*. 1st ed. Netherlands: Springer; 1990.
29. SGU. Product description: Jordarter 1:250 000, nordligaste Sverige. 2014.
30. Hugenholtz CH, Levin N, Barchyn TE, Baddock MC. Remote sensing and spatial analysis of aeolian sand dunes: a review and outlook. *Earth-Sci Rev*. 2012;111(3-4):319-334. doi:10.1016/j.earscirev.2011.11.006
31. Zheng Z, Du S, Taubenböck H, Zhang X. Remote sensing techniques in the investigation of aeolian sand dunes: a review of recent advances. *Remote Sens Environ*. 2022;271(1):112913. doi:10.1016/j.rse.2022.112913
32. Breed CS, Grow T. Morphology and distribution of dunes in sand seas observed by remote sensing. *A Study Global Sand Seas*. 1979;1052:253-302.
33. Ewing RC, Kocurek G, Lake LW. Pattern analysis of dune-field parameters. *Earth Surf Proc Landf J British Geomorphol Res Group*. 2006;31(9):1176-1191. doi:10.1002/esp.1312
34. Fitzsimmons KE, Nowatzki M, Dave AK, Harder H. Intersections between wind regimes, topography and sediment supply: perspectives from aeolian landforms in Central Asia. *Palaeogeogr Palaeoclimatol Palaeoecol*. 2020;540:109531. doi:10.1016/j.palaeo.2019.109531
35. Shumack S, Hesse P, Farebrother W. Deep learning for dune pattern mapping with the AW3D30 global surface model. *Earth Surf Process Landf*. 2020;45(11):2417-2431. doi:10.1002/esp.4888
36. Telfer MW, Fyfe RM, Levin S. Automated mapping of linear dunefield mrphometric parameters from remotely-sensed data. *Aeolian Res*. 2015;19 part B:215-224. doi:10.1016/j.aeolia.2015.03.001
37. Blaschke T. Object based image analysis for remote sensing. *ISPRS J Photogramm Remote Sens*. 2010;65(1):2-16. doi:10.1016/j.isprsjprs.2009.06.004
38. Blaschke T, Feizizadeh B, Hölbling D. Object-based image analysis and digital terrain analysis for locating landslides in the Urmia Lake basin, Iran. IEEE J. *Sel Top Appl Earth Obs Remote Sens*. 2014;7(12):4806-4817. doi:10.1109/JSTARS.2014.2350036
39. Blaschke T, Hay GJ, Kelly M, et al. Geographic object-based image analysis - towards a new paradigm. *ISPRS J Photogramm Remote Sens*. 2014;87(100):180-191. doi:10.1016/j.isprsjprs.2013.09.014
40. Blaschke T, Strobl J. What's wrong with pixels? Some recent developments interfacing remote sensing and GIS. *Geo-Inf-Syst*. 2001;14:12-17.
41. Schneevoigt NJ. Remote sensing in geomorphological and glaciological research. 2012.
42. Schneevoigt NJ, van der Linden S, Thamm HP, Schrott L. Detecting Alpine landforms from remotely sensed imagery. A pilot study in the Bavarian Alps. *Geomorphology*. 2008;93(1-2):104-119. doi:10.1016/j.geomorph.2006.12.034
43. Eisank C, Smith M, Hillier J. Assessment of multiresolution segmentation for delimiting drumlins in digital elevation models. *Geomorphology*. 2014;214(100):452-464. doi:10.1016/j.geomorph.2014.02.028
44. Xiong L, Tang G, Yang X, Li F. Geomorphology-oriented digital terrain analysis: Progress and perspectives. *J Geogr Sci*. 2021;31(3):456-476. doi:10.1007/s11442-021-1853-9
45. Hättestrand C, Götz S, Näslund JO, Fabel D, Stroeven AP. Drumlin formation time: evidence from northern and Central Sweden. *Geogr Ann Ser B*. 2004;86(2):155-167. doi:10.1111/j.0435-3676.2004.00221.x
46. Milne GA, Mitrovica JX, Scherneck H-G, et al. Continuous GPS measurements of postglacial adjustment in Fennoscandia: 2. Modeling results. *J Geophys Res Solid Earth*. 2004;109(B2):B02412. doi:10.1029/2003jb002619
47. Wern L, Bärring L. Sveriges vindklimat 1901-2008 Analys av förändring i geostrofisk vind, Meteorologi Nr 138/2009 SMHI. 2009.
48. Ahlbrandt TS, Andrews S. Distinctive sedimentary features of cold-climate eolian deposits, North Park. *Colorado Palaeogeogr Palaeoclimatol Palaeoecol*. 1978;25(4):327-351. doi:10.1016/0031-0182(78)90048-2
49. Lantmäteriet. *Product description*. Laser data; 2020.
50. Zhang W, Qi J, Wan P, et al. An easy-to-use airborne LiDAR data filtering method based on cloth simulation. *Remote Sens (Basel)*. 2016;8(6):501. doi:10.3390/rs8060501
51. Yan N, Baas ACW. Environmental controls, morphodynamic processes, and ecogeomorphic interactions of barchan to parabolic dune transformations. *Geomorphology*. 2017;278:209-237. doi:10.1016/j.geomorph.2016.10.033
52. Bernhardson M. Aeolian dunes of Central Sweden, Lundqua Thesis. 2018.
53. Hörnberg G, Östlund L, Zackrisson O, Bergman I. The genesis of two Picea-Cladina forests in northernArctic Sweden. *J Ecol*. 1999;87(5):800-814. doi:10.1046/j.1365-2745.1999.00399.x
54. Eisank C, Hölbling D, Friedl B, Chen Y, Chang K-T. Expert knowledge for object-based landslide mapping in Taiwan. South east. *Eur J Earth Obs Geomatics*. 2014;3:347-350.
55. Hölbling D, Friedl B, Eisank C. An object-based approach for semi-automated landslide change detection and attribution of changes to landslide classes in northern Taiwan. *Earth Science Informatics*. 2015;8(2):327-335. doi:10.1007/s12145-015-0217-3
56. Lang S. Object-based image analysis for remote sensing applications: modeling reality—dealing with complexity. In: Blaschke T, Lang S, Hay GJ, eds. *Object-based image analysis; spatial concepts for knowledge-driven remote sensing applications*. Springer; 2008:3-28.
57. Lantmäteriet. Product description: GSD-Elevation data, Grid 2+, Document Version: 2.4 8. 2019.
58. Wessel P. An empirical method for optimal robust regional-residual separation of geophysical data. *Math Geol*. 1998;30(4):391-408. doi:10.1023/A:1021744224009
59. Smith MJ, Clark CD. Methods for the visualization of digital elevation models for landform mapping. *Earth Surf Process Landf*. 2005;30(7):885-900. doi:10.1002/esp.1210
60. Evans IS. Geomorphometry and landform mapping: what is a landform? *Geomorphology*. 2012;137(1):94-106. doi:10.1016/j.geomorph.2010.09.029
61. Favalli M, Fornaciai A. Visualization and comparison of DEM-derived parameters. *Appl Vol Areas Geomorphol*. 2017;290:69-84. doi:10.1016/j.geomorph.2017.02.029
62. Lemenkova P. Topology, homogeneity and scale factors for object detection: application of eCognition software for urban mapping using multispectral satellite image. *Internet Soc*. 2015;80-85. doi:10.6084/m9.figshare.7211588
63. Bishop MP, James LA, Shroder JF, Walsh SJ. Geospatial technologies and digital geomorphological mapping: concepts, issues and research. *Geomorphology*. 2012;137(1):5-26. doi:10.1016/j.geomorph.2011.06.027
64. Chorley RJ, Kennedy BA. *Physical geography: A systems approach*. London: Prentice Hall; 1971.
65. Minár J, Evans IS. Elementary forms for land surface segmentation: the theoretical basis of terrain analysis and geomorphological mapping. *Geomorphology*. 2008;95(3-4):236-259. doi:10.1016/j.geomorph.2007.06.003
66. Hay GJ, Castilla G. Geographic Object-Based Analysis (GEOBIA): A new name for a new discipline. In: Blaschke T, Lang S, Hay GJ, eds. *Object-based image analysis; spatial concepts for knowledge-driven remote sensing applications*. Springer; 2008:75-89. doi:10.1007/978-3-540-77058-9.
67. Levin N, Ben-Dor E, Karnieli A. Topographic information of sand dunes as extracted from shading effects using Landsat images. *Remote Sens Environ*. 2004;90(2):190-209. doi:10.1016/j.rse.2003.12.008
68. Wernette P, Thompson S, Eyler R, et al. Defining dunes: evaluating how dune feature definitions affect dune interpretations from remote

sensing. *J Coast Res*. 2018;34(6):1460. doi:10.2112/jcoastres-d-17-00082.1
69. Graf R, Wegenkittl S. Integration von support vector machines in die objektbasierte Bildklassifizierung am Beispiel der Entwicklung eines plug-ins für eCognition. *Angew Geoinformatik 2012 Beiträge Zum*. 2012;24:52-61.
70. Tzotsos A, Argialas DP. Support Vector Machine Classification for Object-Based Image Analysis. In: Blaschke T, Lang S, Hay GJ, eds. *Object-based image analysis*. Lecture Notes in Geoinformation and Cartography. Berlin Heidelberg: Springer; 2008:V-VIII. doi:10.1007/978-3-540-77058-9.
71. Hussain M, Chen D, Cheng A, Wei H, Stanley D. Change detection from remotely sensed images: from pixel-based to object-based approaches. *ISPRS J Photogramm Remote Sens*. 2013;80:91-106. doi:10.1016/j.isprsjprs.2013.03.006
72. Szuster BW, Chen Q, Borger M. A comparison of classification techniques to support land cover and land use analysis in tropical coastal zones. *Applied Geography*. 2011;31(2):525-532. doi:10.1016/j.apgeog.2010.11.007
73. Hesp PA, Smyth TAG. Nebkha flow dynamics and shadow dune formation. *Geomorphology*. 2017;282:27-38. doi:10.1016/j.geomorph.2016.12.026
74. Sutton SLF, Neuman CMK. Sediment entrainment to the lee of roughness elements: effects of vortical structures. *Case Rep Med*. 2008;113(F2):1-7. doi:10.1029/2007JF000783
75. Bertran P, Andrieux E, Bateman MD, Fuchs M, Klinge M, Marembert F. Mapping and chronology of coversands and dunes from the Aquitaine basin, Southwest France. *Aeolian Research*. 2020;47:100628. doi:10.1016/j.aeolia.2020.100628
76. Seppälä M. Relief control of summer wind direction and velocity: a case study from Finnish Lapland. *Norsk Geografisk Tidsskrift - Norwegian Journal of Geography*. 2002;56(2):117-121. doi:10.1080/002919502760056440
77. Kotilainen MM. *Dune stratigraphy as an indicator of Holocene climatic change and human impact in northern Lapland, Finland*. University of Helsinki; 2004.

SUPPORTING INFORMATION

Additional supporting information can be found online in the Supporting Information section at the end of this article.

How to cite this article: Stammler M, Stevens T, Hölbling D. Geographic object-based image analysis (GEOBIA) of the distribution and characteristics of aeolian sand dunes in Arctic Sweden. *Permafrost and Periglac Process*. 2023;34(1):22-36. doi:10.1002/ppp.2169